Proposed s=±1 octupole bands in ^{140}Xe

Y. Huang (□□), S. J. Zhu (□□□), J. H. Hamilton, E. H. Wang, A. V. Ramayya, Z. G. Xiao (□□□), H. J. Li (□□□), Y. X. Luo, J. O. Rasmussen, G. M. Ter-Akopian, and Yu. Ts. Oganessian

Phys. Rev. C **93**, 064321 — Published 20 June 2016

DOI: 10.1103/PhysRevC.93.064321

Proposed $s = \pm 1$ octupole bands in ^{140}Xe

Y. Huang(黄彦),[1] S. J. Zhu(朱胜江),[1,*] J. H. Hamilton,[2] E. H. Wang,[2] A. V. Ramayya,[2] Z. G. Xiao(肖志刚),[1] H. J. Li(李红洁),[1] Y. X. Luo,[2,3] J. O. Rasmussen,[3] G. M. Ter-Akopian,[4] and Yu. Ts. Oganessian[4]

[1]*Department of Physics, Tsinghua University, Beijing 100084, People's Republic of China*
[2]*Department of Physics, Vanderbilt University, Nashville, Tennessee 37235 USA*
[3]*Lawrence Berkeley National Laboratory, Berkeley, California 94720 USA*
[4]*Joint Institute for Nuclear Research, Ru-141980 Dubna, Russia Federation*

Level structures of neutron-rich ^{140}Xe nucleus have been reinvestigated by using a triple γ coincidence study from the spontaneous fission of ^{252}Cf. Several new levels and transitions are identified. The previously observed $s = +1$ octupole band structure is confirmed and expanded. Another set of the $\triangle I = 2$ positive- and negative- parity bands connected by strong $E1$ transitions is proposed as the $s = -1$ octupole band structure. Thus, the $s = \pm 1$ doublet octupole bands are completed in ^{140}Xe. The experimental $B(E1)/B(E2)$ branching ratios indicate that the octupole correlations in ^{140}Xe are weak. The other characteristics of the $s = \pm 1$ octupole bands have been discussed.

PACS numbers: 21.10.Re, 23.20.Lv, 27.60.+j, 25.85.Ca

I. INTRODUCTION

Nuclear deformation is a manifestation of collective motion mode in nuclei. The occurrence of octupole deformation characterizing the reflection asymmetry of the nuclear shape has drawn increasingly extensive attention for its relevance to the violation of fundamental symmetries in nuclei [1–4]. In the language of random-phase approximation (RPA) with separable multipole interactions in the Hamiltonian, the octupole deformation originates from a parity-breaking odd-multipolarity interaction which couples intrinsic states of opposite parity near the Fermi surface. The stability or softness of the octupole deformation depends on the octupole coupling constant. With a coupling constant smaller than the critical value, octupole vibration is shown instead of static octupole deformation. Because of the fluctuation associated with the finite-size effect of nuclei, the barrier sustaining the static octupole deformation is reduced. It results in the octupole correlations featuring a smooth and continuous pattern of the reflection asymmetric deformation parameter [4]. Strong octupole deformation/correlations can be expected if nucleons near the Fermi surface occupy states of opposite parity with orbital and total angular momentum differing by $3\hbar$. Namely, such conditions can be satisfied in the regions with neutron or proton numbers near 34, 56, 88 and 134 where both the intruder subshell (l,j) and the normal-parity subshell ($l-3$,$j-3$) with $\Delta N = 1$ are present in the vicinity of the Fermi surface.

Experimental evidence of octupole correlations lies in the appearance of strong E1 transitions between two opposite parity bands with interspacing energy levels. Generally, the level pattern of the rotational bands in reflection-asymmetric nuclei can be characterized by the simplex quantum number s, which is defined as the eigenvalue of the compound operator combining the space inversion (parity) operation and the rotation by 180° with respect to the principle axis [5]. For even-even nuclei, two sets of parity doublet bands with $s = \pm 1$ are expected corresponding to the two sequences following $I^\pi = 0^+, 1^-, 2^+, 3^-, \cdots$ ($s = +1$) and $I^\pi = 0^-, 1^+, 2^-, 3^+, \cdots$ ($s = -1$), respectively. While for odd-A nuclei, $s = \pm i$ are expected corresponding to $I^\pi = 1/2^+, 3/2^-, 5/2^+, 7/2^-, \cdots$ ($s = +i$) and $I^\pi = 1/2^-, 3/2^+, 5/2^-, 7/2^+, \cdots$ ($s = -i$), respectively.

Early examples of octupole deformation/correlations were reported in some even-even nuclei in several mass regions, including ^{150}Sm [6], $^{150-152}$Gd [7, 8] in $N \approx 88$ samarium-gadolinium region, ^{142,144,146}Ba isotopes of $Z = 56$ and $N \approx 88$ [9], as well as ^{218}Ra [10] and ^{222}Th [11, 12] in radium-thorium mass region with $Z \approx 88$ and $N \approx 134$. With the development of large detector arrays utilized in prompt γ spectroscopy following fission of heavy nuclei [13], more abundant examples of octupole deformation/correlations are identified in $^{140-146,148}$Ba ($Z = 56$) [13–17], ^{145,147}La ($Z = 57$) [18] and $^{144,146-148,150,152}$Ce (Z =58) [13, 19–26]. Among these nuclei, most of the octupole bands were observed with a single simplex quantum number, namely $s = +1$ band structure in even-even nuclei and $s = +$ i or $s =$ -i band structure in odd-A nuclei. The experimental result of two sets of parity doublet bands with the double simplex values originated from a same configuration is very scarce. It was only observed in a few nuclei, for example, in even-even ^{148}Ce with $s = \pm 1$ [23] and in odd-A ^{143}Ba with $s = \pm$ i [17].

The neutron-rich even-even ^{140}Xe nucleus with $Z = 54$, $N = 86$ is located at the lower edge of the $Z = 56$, $N = 88$ octupole deformed island. Search for the octupole band structures in this nucleus is important for systematically understanding the characteristics of the octupole deformation and octupole correlations in this region. In previous publications [13, 27, 28], the high spin level struc-

*Electronic address: zhushj@mail.tsinghua.edu.cn

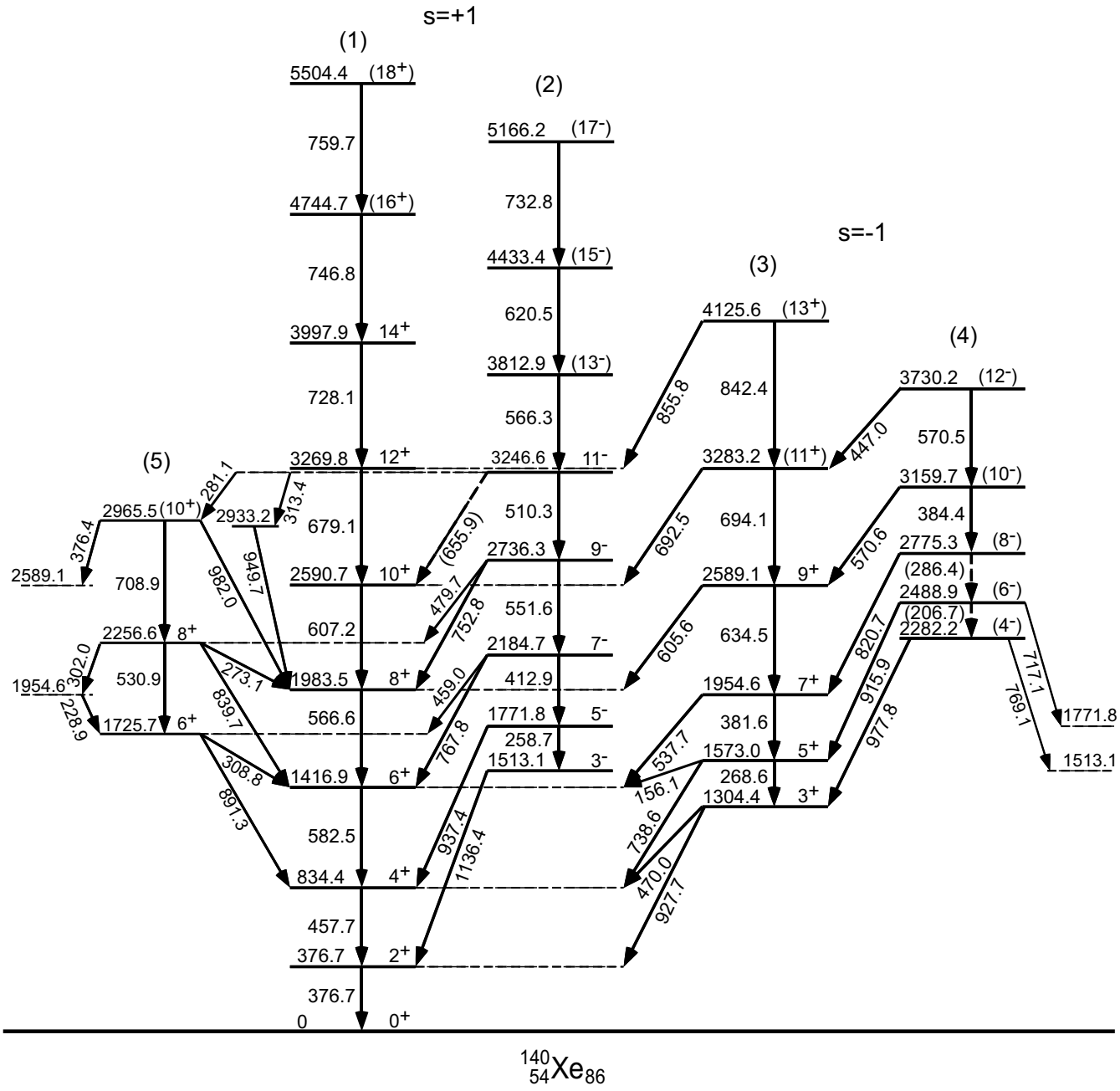

FIG. 1: The level scheme of ^{140}Xe identified in present work.

tures in ^{140}Xe have been established. Then, the $s = +1$ octupole band structure was reported in [29]. In this paper, we reinvestigate the high-spin states in ^{140}Xe. The octupole bands are significantly expanded and the $s = \pm 1$ doublet octupole bands are identified. Since this work was submitted, a new study of ^{140}Xe has been recently published [30].

II. EXPERIMENTS AND RESULTS

The level structures of ^{140}Xe in the present work were investigated through measuring the prompt γ-rays emitted from the fragments produced in the spontaneous fission of ^{252}Cf. The experiment was carried out at the Lawrence Berkeley National Laboratory using a ^{252}Cf source of strength ~ 60 μCi. The source was sandwiched between two Fe foils of thickness of 10 mg/cm^2. The Gammasphere detector array, consisting of 101 Compton-suppressed Ge detectors in this time, was used to detect the γ rays. A total of 5.7×10^{11} triple-

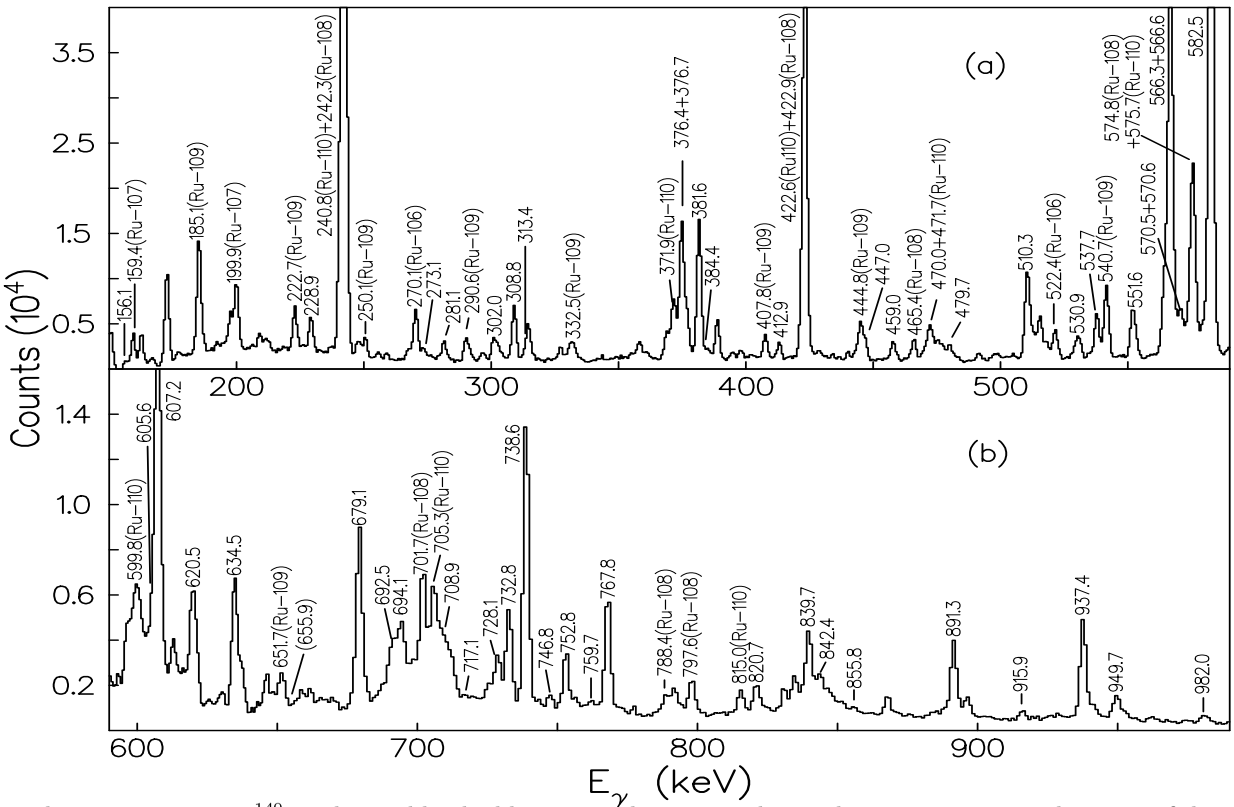

FIG. 2: The γ-ray spectra in ^{140}Xe obtained by double gate on the 376.7 and 457.7 keV γ transitions. The range of the energy is (a) from 150 to 590 keV, and (b) from 590 to 990 keV.

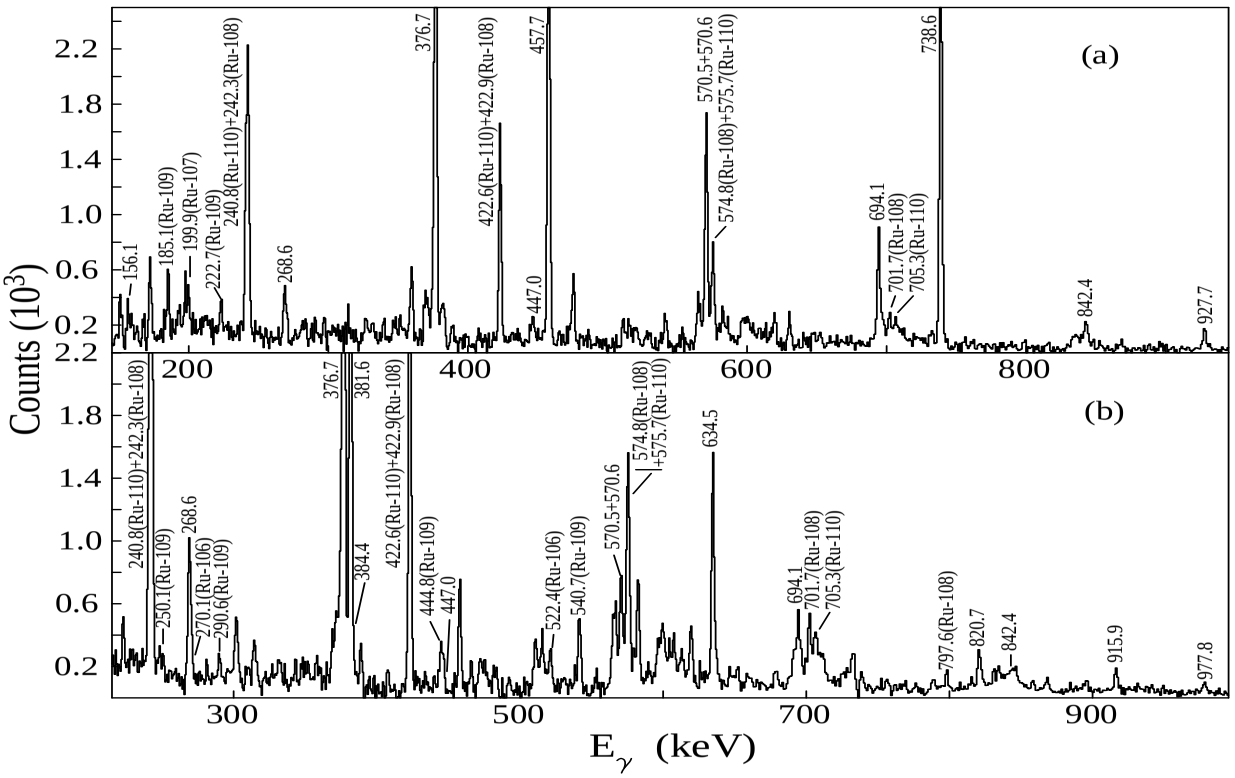

FIG. 3: Partial γ-ray spectra in ^{140}Xe by (a) duoble gates on the 381.6 and 634.5 keV γ transitions, and (b) by summing double gating on 376.7 and 927.7 keV, and 457.7 and 738.6 keV γ-transitions.

and higher fold γ-coincidence events were collected. A γ-γ-γ coincidence matrix (cube) were constructed. Detailed information of the experiment can be found in Refs. [13, 23–25]. The coincidence data were analyzed with the Radware software package [31].

The level scheme of ^{140}Xe obtained from the present work is shown in Fig. 1. Five collective band structures with $\Delta I = 2$ transitions are labeled on top of the bands with numbers (1)-(5). Most of the levels and transitions reported in Refs. [13, 27–29] are confirmed in this work. Some new levels and transitions are added to the scheme. Bands (1) and (2) have been identified up to the 5504.4 keV and 4433.4 keV levels, respectively, in Ref. [29]. We add a new level at 5166.2 keV along with a new transition of 732.8 keV in band (2) as new also reported in Ref. [30]. Bands (3) - (4) are newly assigned in this work. They were not reported in Ref. [29], but some levels and transitions in these bands have been observed in earlier reports [13, 27, 28]. Here we have identified some new levels and transitions in these two bands, for examples, a level at 4125.6 keV and a transition of 842.4 keV in band (3), two levels at 2282.2 and 2488.9 keV in band (4). Both bands (3) and (4) are also reported in Ref. [30], but the 2282.2 and 2488.9 keV levels in band (4) are not reported in Ref. [30]. In addition, a level at 2965.5 keV and a transition of 708.9 keV in band (5) is newly found and also reported in Ref. [30]. Besides, some linking transitions between the bands are also newly identified. The levels at 3704.6 and 1433.0 keV along with some weak transitions reported in Ref. [30] are not observed in this work. A summary of the γ-transition energies, relative intensities, multipolarities, and spin and parity (I^π) assignments in ^{140}Xe are given in Table I. The γ-transition intensities have been normalized to that of the 376.7 keV ($2^+ \rightarrow 0^+$) γ ray.

TABLE I: The energies, relative intensities, multipolarities, and spin and parity (I^π) assignments of the γ-transitions and levels in ^{140}Xe.

E_γ(keV)	Int.(%)	E_i(keV)	→	E_f(keV)	Assignment	Mult.
156.1	0.48(4)	1573.0	→	1416.9	$5^+ \rightarrow 6^+$	$M1/E2$
(206.7)	(<0.1)	2488.9	→	2282.2	$(6^-) \rightarrow (4^-)$	$(E2)$
228.9	1.07(9)	1954.6	→	1725.7	$7^+ \rightarrow (5^+)$	$(E2)$
258.7	0.37(5)	1771.8	→	1513.1	$5^- \rightarrow 3^-$	$E2$
268.6	1.37(7)	1573.0	→	1304.4	$5^+ \rightarrow 3^+$	$E2$
273.1	0.94(3)	2256.6	→	1983.5	$8^+ \rightarrow 8^+$	$(M1/E2)$
281.1	0.34(4)	3246.6	→	2965.5	$11^- \rightarrow 10^+$	$E1$
(286.4)	(<0.1)	2775.3	→	2488.9	$(8^-) \rightarrow (6^-)$	$(E2)$
302.0	0.74(4)	2256.6	→	1954.6	$8^+ \rightarrow 7^+$	$(M1/E2)$
308.8	2.92(6)	1725.7	→	1416.9	$6^+ \rightarrow 6^+$	$(M1/E2)$
313.4	0.70(3)	3246.6	→	2933.2	$11^- \rightarrow$	
376.4	0.29(2)	2965.5	→	2589.1	$10^+ \rightarrow 9^+$	$M1$
376.7	100.0	376.7	→	0	$2^+ \rightarrow 0^+$	$E2$
381.6	6.35(26)	1954.6	→	1573.0	$7^+ \rightarrow 5^+$	$E2$
384.4	0.36(2)	3159.7	→	2775.3	$(10^-) \rightarrow (8^-)$	$(E2)$
412.9	1.00(7)	2184.7	→	1771.8	$7^- \rightarrow 5^-$	$E2$
447.0	0.25(5)	3730.2	→	3283.2	$(12^-) \rightarrow (11^+)$	$(E1)$
457.7	87.1(4)	834.4	→	376.7	$4^+ \rightarrow 2^+$	$E2$
459.0	0.73(5)	2184.7	→	1725.7	$7^- \rightarrow 6^+$	$E1$
470.0	2.73(4)	1304.4	→	834.4	$3^+ \rightarrow 4^+$	$M1$
479.7	1.68(7)	2736.3	→	2256.6	$9^- \rightarrow 8^+$	$E1$
510.3	3.46(11)	3246.6	→	2736.3	$11^- \rightarrow 9^-$	$E2$
530.9	2.29(5)	2256.6	→	1725.7	$8^+ \rightarrow 6^+)$	$(E2)$
537.7	3.03(6)	1954.6	→	1416.9	$7^+ \rightarrow 6^+$	$M1/E2$
551.6	5.46(26)	2736.3	→	2184.7	$9^- \rightarrow 7^-$	$E2$
566.3	2.11(9)	3812.9	→	3246.6	$(13^-) \rightarrow 11^-$	$(E2)$
566.6	35.6(2)	1983.5	→	1416.9	$8^+ \rightarrow 6^+$	$E2$
570.5	0.44(4)	3730.2	→	3159.7	$(12^-) \rightarrow (10^-)$	$(E2)$
570.6	1.78(5)	3159.7	→	2589.1	$(10^-) \rightarrow 9^+$	$(E1)$
582.5	52.5(3)	1416.9	→	834.4	$6^+ \rightarrow 4^+$	$E2$
605.6	3.32(30)	2589.1	→	1983.5	$9^+ \rightarrow 8^+$	$M1/E2$
607.2	16.9(2)	2590.7	→	1983.5	$10^+ \rightarrow 8^+$	$E2$
620.5	1.12(6)	4433.4	→	3812.9	$(15^-) \rightarrow (13^-)$	$(E2)$
634.5	4.70(10)	2589.1	→	1954.6	$9^+ \rightarrow 7^+$	$E2$

TABLE I: Continue.

E_γ(keV)	Int.(%)	E_i(keV)	→	E_f(keV)	Assignment	Mult.
(655.9)	(<0.1)	3246.6	→	2590.7	$11^- \rightarrow 10^+$	$E1$
679.1	7.25(11)	3269.8	→	2590.7	$12^+ \rightarrow 10^+$	$E2$
692.5	1.36(5)	3283.2	→	2590.7	$(11^+) \rightarrow 10^+$	$(M1/E2)$
694.1	1.61(6)	3283.2	→	2589.1	$(11^+) \rightarrow 9^+$	$(E2)$
708.9	<0.1	2965.5	→	2256.6	$(10^+) \rightarrow 8^+$	$(E2)$
717.7	0.13(2)	2488.9	→	1771.8	$(6^-) \rightarrow 5^-$	$(M1/E2)$
728.1	1.85(6)	3997.9	→	3269.8	$14^+ \rightarrow 12^+$	$E2$
732.8	0.84(5)	5166.2	→	4433.4	$(17^-) \rightarrow (15^-)$	$(E2)$
738.6	12.1(2)	1573.0	→	834.4	$5^+ \rightarrow 4^+$	$M1/E2$
746.8	0.76(3)	4744.7	→	3997.9	$(16^+) \rightarrow 14^+$	$(E2)$
752.8	4.24(10)	2736.3	→	1983.5	$9^- \rightarrow 8^+$	$E1$
759.7	0.34(2)	5504.4	→	4744.7	$(18^+) \rightarrow (16^+)$	$(E2)$
767.8	5.11(10)	2184.7	→	1416.9	$7^- \rightarrow 6^+$	$E1$
769.1	0.49(5)	2282.2	→	1513.1	$(4^-) \rightarrow 3^-$	$(M1/E2)$
820.7	1.21(6)	2775.3	→	1954.6	$(8^-) \rightarrow 7^+$	$(E1)$
839.7	3.21(8)	2256.6	→	1416.9	$8^+ \rightarrow 6^+$	$(M1/E2)$
842.4	0.55(4)	4125.6	→	3283.2	$(13^+) \rightarrow (11^+)$	$(E2)$
855.8	0.15(2)	4125.6	→	3269.8	$(13^+) \rightarrow 12^+$	$(M1/E2)$
891.3	4.16(7)	1725.7	→	834.4	$6^+ \rightarrow 4^+$	$(M1/E2)$
915.9	0.38(2)	2488.9	→	1573.0	$(6^-) \rightarrow 5^+$	$(E1)$
927.7	3.88(10)	1304.4	→	376.7	$3^+ \rightarrow 2^+$	$M1/E2$
937.4	5.24(8)	1771.8	→	834.4	$5^- \rightarrow 4^+$	$E1$
949.7	1.47(6)	2933.2	→	1983.5	$\rightarrow 8^+$	
977.8	0.35(3)	2282.2	→	1304.4	$4^- \rightarrow 3^+$	$(E1)$
982.0	<0.1	2965.5	→	1983.5	$(10^+) \rightarrow 8^+$	$(M1/E2)$
1136.4	1.67(7)	1513.1	→	376.7	$3^- \rightarrow 2^+$	$E1$

As examples, Figs. 2 and 3 present some coincidence γ-ray spectra in ^{140}Xe. In Fig. 2, by double gating on the 376.7 and 457.7 keV γ transitions in band (1), all the corresponding transitions above the 834.4 keV level in Fig. 1 can be seen. Figure 3 (a) is generated by double gating on the 381.6 and 634.5 keV γ transitions in band (3). In addition to the γ transitions below 1573.0 keV (5^+) level, such as, 268.6 keV in band (3), 376.7 and 457.7 keV in band (1), and 927.7, 738.6 and 156.1 keV between bands (2) and (3), one can see the 694.1 and 842.4 keV γ peaks in band (3), 570.5 keV (mixed with 570.6 keV) γ peak in band (4), and 570.6 and 447.0 keV γ peaks between bands (3) and (4). Fig. 3(b) shows a partial coincidence spectrum with summing double gating on 376.7 and 927.7 keV, and 457.7 and 738.6 keV γ-transitions. In this spectrum, all the γ peaks in bands (3) and (4) as well as the linking transitions between bands (3) and (4) can been seen. From these spectra, one can also see some partner γ peaks, such as, 240.8, 371.9, 422.6, 471.7, 575.7, 599.8, 705.3 and 815.0 keV in ^{110}Ru (2n) [32], 185.1, 222.7, 250.1, 290.6, 332.5, 407.8 444.8, 540.7 and 651.7 keV in ^{109}Ru (3n) [33], 242.3, 422.9, 465.6, 574.8, 701.7, 786.4 and 797.6 keV in ^{108}Ru (4n) [32], 159.4 and 199.9 keV in ^{107}Ru (5n) [34], and 270.1 and 522.4 keV in ^{106}Ru (6n) [35] in addition to the γ peaks observed in ^{140}Xe.

The spin and parity (I^π) for the levels in bands (1) and (2) were assigned in Ref. [29]. The yrast band (1) belongs to a positive parity band and the side band (2) is a negative parity band. These two bands, with in-band $\Delta I = 2$ transitions in each one and linking $E1$ transitions in between form an octupole band structure with simplex quantum number $s = +1$ in ^{140}Xe, as already reported in [29]. Our experimental results are consistent with that assignment. Based on the observed structural

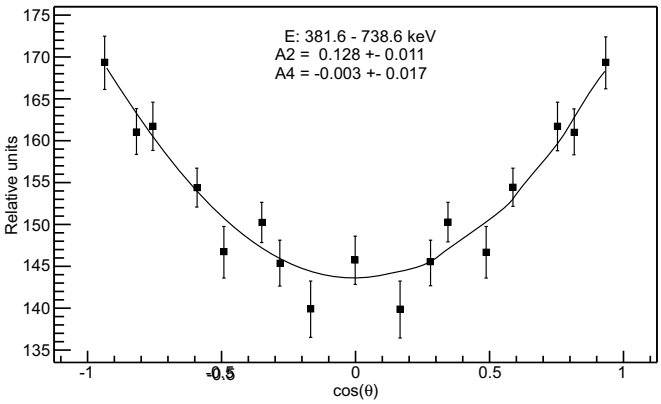

FIG. 4: Angular correlations for 381.6→738.6 keV cascade in ^{140}Xe.

characteristics in present work including our angular correlation work and that of Ref. [30], we assign band (3) as a positive parity band as also assigned in Ref. [30] and tentatively band (4) as a negative parity band. Thus, another set of doublets consisting of a positive parity band (3) and a negative parity band (4) forms an octupole band structure with simplex quantum number s = - 1 in ^{140}Xe, provided that the linking $E1$ transitions and the interspacing levels of alternating parities appear between these two bands. Then we can see that two sets of positive- and negative-parity bands (1) and (2), and bands (3) and (4) form the complete $s = \pm 1$ octupole bands in ^{140}Xe.

In order to confirm the assignments mentioned above, the $\gamma \rightarrow \gamma(\theta)$ angular correlation measurements have been carried out by dividing the data set into angular bins [36]. Because most of the non-yrast transitions in ^{140}Xe are very weak, we only obtained several angular correlation values in ^{140}Xe. As an example, Fig. 4 shows the experimental angular correlation curve for the 381.6→738.6 keV cascade. The obtained A_2 and A_4 values are 0.128(11) and -0.003(17), respectively, and yield for the $7^+(E2)5^+(M1/E2)4^+$ cascade a mixing ratio δ(E2/M1)=0.51(4) (see Table II). Our experimental $\gamma-\gamma(\theta)$ results and extracted δ values [36] and some comparison with theoretical values [37] are given in Table II and form the bases for the discussion below. These data offer further support for the I^π assignments of ^{140}Xe in the present work.

III. DISCUSSION

In Table II the δ(Q/D) values for the 738.6 keV transition are 0.51 (4) or 3.0 (3) from the $7^+-5^+-4^+$ $\gamma-\gamma(\theta)$. The A_2 and A_4 values of Ref. [30] agree very nicely with our values. We also measured 738.6 457.7 keV $\gamma-\gamma(\theta)$ and found the 738.6 keV transition δ = 0.53(3) or 1.6 (1) (the latter only if you allow an unlikely 3σ variation on A_4). The only consistent results is the 738.6 keV, 5^+-4^+ transition is 80% dipole and 20% quadrupole as also given in Ref. [30].

The δ values for the 537.7 keV, 7^+ - 6^+ transition from the 537.7 582.5 and 537.7 457.7 $\gamma-\gamma(\theta)$ are both pure dipole or pure quadrupole. The δ values for 3^+ - 2^+, 927.7 keV transition from the 3^+ - 2^+ -0^+ $\gamma-\gamma(\theta)$ are 0.55 (9) or 1.3 (2) to give 80%(D)/20%(Q) or 28%(D)/72%(Q). Our A_2 and A_4 values agree with those of Ref. [30]. So the 738.6 keV, 5^+ - 4^+ and 927.7 keV, 3^+ - 2^+ transition are clearly 80% dipole radiation and the 7^+ - 6^+ transition is either pure dipole or pure quadrupole. If the 3^+ and 5^+ levels were members of a γ-vibrational band, then their transitions should be 90-100% E2 transitions as expected in the Bohr-Mottelson model. From ^{150}Sm through ^{184}W, the gamma band to ground band transitions are all essentially pure E2 (see Ref. [38]. In the most accurate case of ^{166}Er, the δ values are -16 to -35 from 2_γ 2_g to 7_γ - 8_g (Ref. [38]). More recently, the γ band to ground transition accurate δ values in ^{102}Mo (to 3_γ 2_g), ^{104}Mo (to 7_γ 6_g), ^{106}Mo (to 7_γ 6_g) yield $92-100$% E2 and in ^{108}Ru (to 3_γ 2_g), ^{110}Ru (to 5_γ 4_g), ^{112}Ru (to 3_γ 2_g), yield $98-100$% E2 [39]. Then the interpretation of bands (3) and (5) in our figure (Fig. 1) as forming a γ vibrational band is not supported by the multipolarities of the $\Delta I = 0, 1$ transitions.

Also the δ (308.8 keV, 6^+ - 6^+ transition) is 0.43 (8) in our work and is given as 0.48 (4) in Ref. [30]. So this large 85% dipole radiation for this transition is clearly not consistent with the upper 6^+ state being a member of a γ band. Thus, we reject the interpretation [30] of our bands (3) and (5) as forming a γ-vibrational band. The most consistent interpretation is bands (3) and (4) form a s = -1 octupole band as shown in Fig. 1 in line with similar octupole bands with s = -1 and -i in ^{148}Ce and ^{143}Ba (see Fig. 5) and the similar δ(E) values for the s = +1 and -1 bands in ^{140}Xe (see Fig. 6).

Now we discuss the characteristics of the $s = \pm 1$ octupole bands in ^{140}Xe. Fig. 5 shows a comparison of observed levels for the $s = \pm 1$ octupole bands in even-even ^{140}Xe and ^{148}Ce [23], and for the $s = \pm i$ octupole bands in odd-A ^{143}Ba [17]. They show very similar characteristics with each other. This indicates that the assigned $s = \pm 1$ octupole bands in ^{140}Xe is reasonable. On the other hand, from Fig. 5 one can see that the level energies with the same spin in ^{140}Xe are higher than those in ^{148}Ce. This is caused by the variation of the quadrupole deformation parameter (β_2). The β_2 value in ^{140}Xe should be less than that in ^{148}Ce.

In a nuclear octupole band structure, the $B(E1)/B(E2)$ branching ratios can been obtained via

$$\frac{B(E1)}{B(E2)} = 0.771 \frac{I_\gamma(E1)}{I_\gamma(E2)} \frac{E_\gamma(E2)^5}{E_\gamma(E1)^3} (10^{-6} \cdot fm^{-2}) \quad (1)$$

where the intensities (I_γ) and energies (E_γ) in ^{140}Xe are taken from the present data. The $B(E1)/B(E2)$ values in ^{140}Xe from our investigation are listed in Table III. With the new intensities in Ref. [30] and our recalculation of the intensity of the 551 keV transition, the $B(E1)/B(E2)$ ratio for the first three can differ by about 30% and in agreement with one σ in one case. In the present work, the average $B(E1)/B(E2)$ value for the $s = \pm 1$ octupole bands in ^{140}Xe is 0.132 $\times(10^{-6}\cdot$fm$^{-2})$. The average $B(E1)/B(E2)$ values for $s = \pm i$ octupole bands in ^{143}Ba [17] and $s = \pm 1$ octupole bands in ^{148}Ce [23] are 0.78 and 1.07 $\times(10^{-6}\cdot fm^{-2})$, respectively. These data show that the observed octupole correlations of the double octupole bands in ^{140}Xe are much weaker than those in ^{143}Ba and ^{148}Ce.

The energy differences δE between the positive- and the negative-parity bands in an octupole band structure reflect the octupole deformation stability varying with spin. The δE values can be calculated from the experimental level energies by using the relation [23, 24]

$$\delta E(I) = E(I^\pm) - \frac{(I+1)E(I-1)^\mp + IE(I+1)^\mp}{2I+1} \quad (2)$$

TABLE II: Angular correlations for some cascade transitions and the spin and parity assignments for the levels as well as the mixing ratios for some $M1/E2$ transitions in ^{140}Xe. Some mixing ratios δ are calculated from the average of the current data and Ref. [30]. Ref. [30] reported A_2 as 0.204 for the 309-sum $\gamma - \gamma(\theta)$. However, the δ values of 0.48 and -0.23 in Ref. [30] for the 6-6-4 and 5-6-4 spins are consistent only with an A2 of 0.050 and 0.054, respectively, which are in agreement with our A2=0.064(23).

Cascade (keV)	$A_2^{exp.}$	$A_4^{exp.}$	$A_2^{th.}$	$A_4^{th.}$	$\delta(E2/M1)$	Assignment
728.1-679.1	0.118(27)	0.001(41)	0.102	0.009		$14^+(E2)12^+(E2)10^+$
927.7-376.7	0.203(22)	-0.070(34)			0.55(9) or 1.3(2)	$3^+(M1/E2)2^+(E2)0^+$
	0.254(23)[a]	0.058(43)[a]				
738.6-457.7	0.203(8)	0.003(13)			0.53(3) or 1.6(1) for 3σ on A_4	$5^+(M1/E2)4^+(E2)2^+$
738.6-sum[a]	0.189(5)	-0.017(8)				
381.6-738.6	0.128(11)	-0.003(17)			0.51(4) or 3.0(3)	$7^+(E2)5^+(M1/E2)4^+$
	0.126(5)[a]	-0.009(8)[a]				
537.7-582.5	-0.066(34)	0.019(53)	-0.071	-0.000	0 or 18 for 1.5σ on A_4	$7^+(M1/E2)6^+(E2)4^+$
537.7-457.7	-0.086(23)	0.002(35)	-0.071	-0.000	0 or 40 for 1.5σ on A_4	$7^+(M1/E2)6^+, 4^+(E2)2^+$
634.5-381.0	0.094(17)	0.008(27)	0.102	0.009		$9^+(E2)7^+(E2)5^+$
	0.099(13)[a]	0.037(22)[a]	0.102	0.009		$9^+(E2)7^+(E2)5^+$
891.3-457.7	0.117(25)	-0.014(39)	0.102	0.009		$6^+(E2)4^+(E2)2^+$
891.3-sum[a]	0.100(35)	0.065(58)	0.102	0.009		$6^+(E2)4^+(E2)2^+$
839.7-582.5	0.116(32)	0.003(49)	0.102	0.009		$8^+(E2)6^+(E2)4^+$
308.8-582.5	0.064(23)	-0.005(36)			0.43(8) or -1.5(2) for 2σ on A_4	$6^+(M1/E2)6^+(E2)4^+$

[a]Result from Ref. [30]

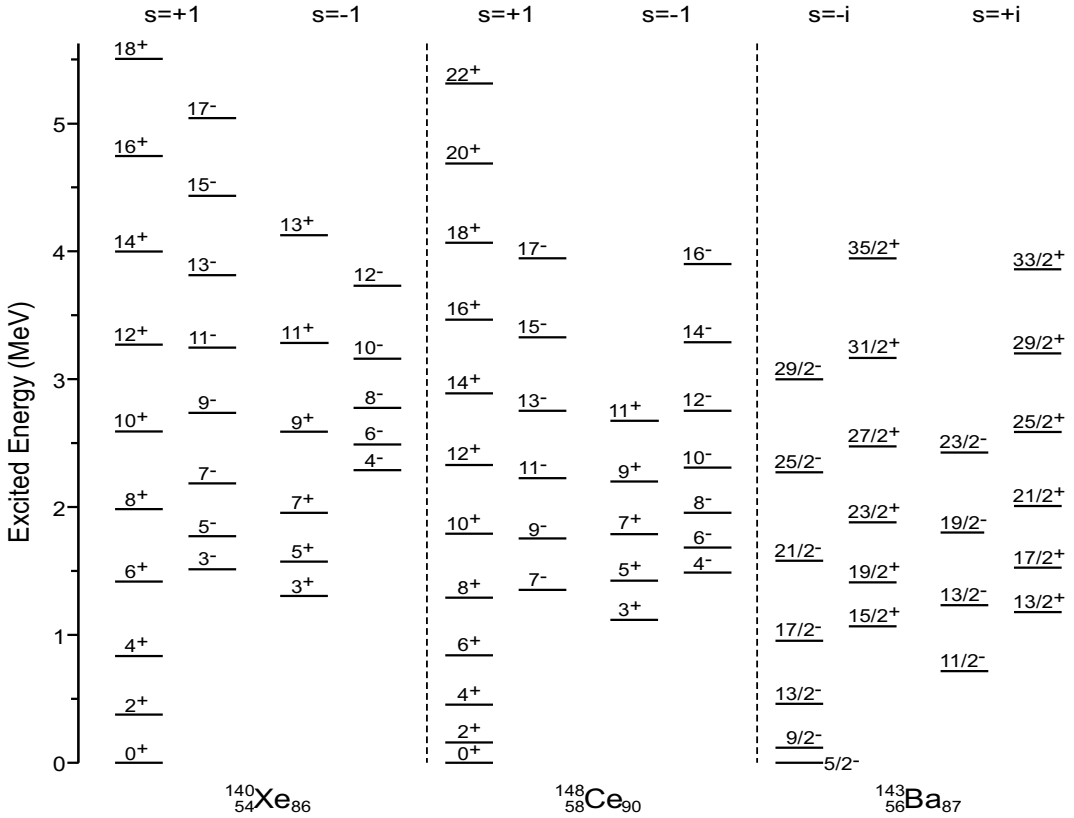

FIG. 5: Systematic comparisons for the levels of $s = \pm 1$ octupole bands in ^{140}Xe, ^{148}Ce [23] and $s = \pm i$ octupole bands in ^{143}Ba [17].

TABLE III: $B(E1)/B(E2)$ branching ratios in ^{140}Xe.

Simplex	E_γ(keV)	$I_i^\pi \to I_f^\pi$	I_γ	$\frac{B(E1)}{B(E2)}10^{-6}fm^{-2}$	
$s=+1$	937.4	$5^- \to 4^+$	5.24(8)	0.015(3)	0.02(1)[a]
bands(1)	258.7	$5^- \to 3^-$	0.37(5)		
and (2)	767.8	$7^- \to 6^+$	5.11(10)	0.104(8)	0.068(5)[a]
	412.9	$7^- \to 5^-$	1.00(7)		
	752.8	$9^- \to 8^+$	3.19(8)	0.072(4)	0.047(5)[a]
	551.6	$9^- \to 7^-$	1.94(6)		
$s=-1$	570.6	$10^- \to 9^+$	1.78(5)	0.17(1)	0.17(6)[a]
bands(3)	384.4	$10^- \to 8^-$	0.36(2)		
and (4)	447.0	$12^- \to 11^+$	0.25(5)	0.30(7)	0.9(6)[a]
	570.5	$12^- \to 10^-$	0.44(4)		

[a]Calculated from the intensities reported in Ref. [30].

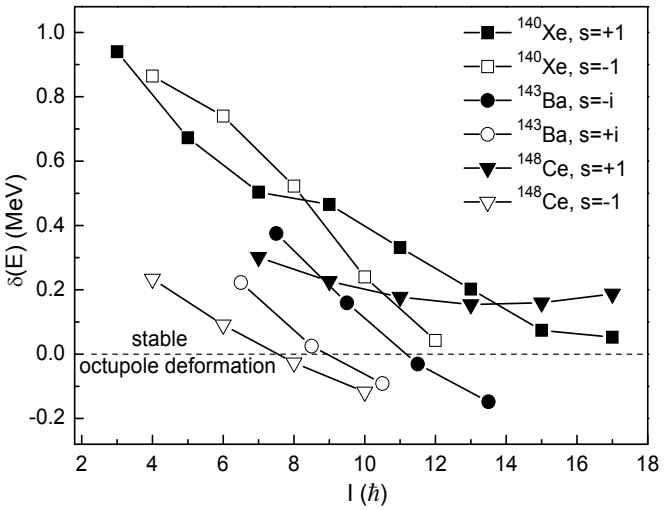

FIG. 6: The comparison for $\delta E(I)$ versus spin I for $s=\pm1$ octupole bands in ^{140}Xe, ^{148}Ce [23] and $s=\pm i$ octupole bands in ^{143}Ba [17].

Here the superscripts indicate the parities of the levels. Figure 6 shows the plots of the $\delta E(I)$ as a function of the spin I of the $s=\pm1$ octupole bands in ^{140}Xe, ^{148}Ce [23] and the $s=\pm i$ octupole bands in ^{143}Ba [17]. In the limit of stable octupole deformation, $\delta E(I)$ should be close to zero. As seen in Fig. 6, the $\delta E(I)$ decreases with the spin I in each octupole band. It is close to the stable point at $I\sim 7.5$, 9, 11 and 12 $\hbar$ for $s=-1$ in ^{148}Ce, $s=+i$ in ^{143}Ba, $s=-i$ in ^{143}Ba and $s=-1$ band structures in ^{140}Xe, respectively. But for $s=+1$ bands in ^{140}Xe and ^{148}Ce, they do not quite reach the stable point up to spin 17 $\hbar$. This result shows that the octupole correlation in ^{140}Xe is less stable than that in ^{143}Ba and ^{148}Ce. On the other hand, the $\delta E(I)$ as a function of spin for the $s=+1$ band structure in ^{148}Ce exhibits differently more gentle variation than others.

The kinematic moments of inertia (J_1) against the rotation frequencies ($\hbar\omega$) for the $s=\pm1$ octupole bands in

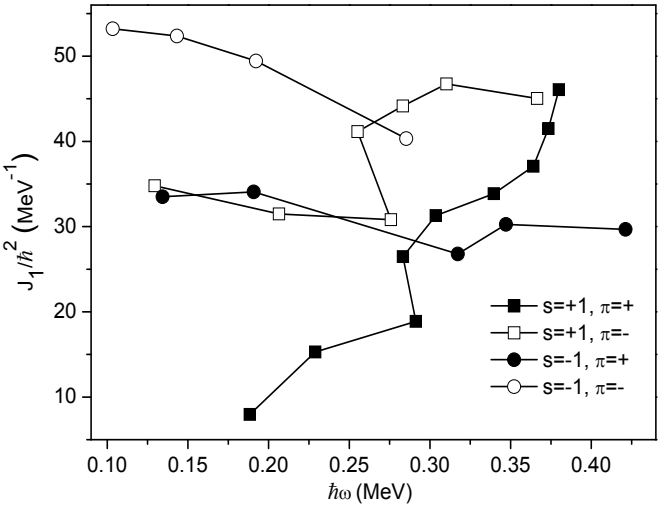

FIG. 7: Moments of inertia (J_1) as a function of the rotation frequency ($\hbar\omega$) for $s=\pm1$ octupole bands in ^{140}Xe.

^{140}Xe are plotted in Fig. 7. One can see the J_1 curves for the $\Delta I=2$ bands show rather different behaviors. At the lower rotational frequency ($\hbar\omega<0.27$ MeV), the J_1 values are the smallest for the $s=+1$, $\pi=+$ band, medium for $s=+1$, $\pi=-$ and $s=-1$, $\pi=+$ bands, and the largest for $s=-1$, $\pi=-$ band, respectively. The curve increases with $\hbar\omega$ for $s=+1$, $\pi=+$ band and $\pi=-$ band but decreases with $\hbar\omega$ for the $s=-1$ bands. Similar J_1 characteristics are also shown in $s=\pm1$ octupole bands in ^{148}Ce [23]. Moreover, with the increasing of the frequency $\hbar\omega$, backbending occurs for both the positive and the negative parity bands of the $s=+1$ octupole band structure at $\hbar\omega\approx 0.25-0.3$ MeV in ^{140}Xe. This backbending should be caused by the alignments of a pair of protons or neutrons.

The characteristics for the side band (5) in ^{140}Xe are not clear yet, and more work is needed to understand it.

IV. SUMMARY

In the present work, the high spin states in the neutron-rich ^{140}Xe nucleus have been reinvestigated. The previously observed $s=+1$ octupole band structure is confirmed and expanded. A new $s=-1$ octupole band structure has been proposed and so the $s=\pm1$ doublet octupole bands are completed in ^{140}Xe. The observed $B(E1)/B(E2)$ branching ratios indicate that the octupole correlations in ^{140}Xe are weak. The energy difference of the successive levels of alternating parities and the kinetic moments of the inertia of the $s=\pm1$ octupole bands are discussed.

Acknowledgments

The work at Tsinghua University was supported by the National Natural Science Foundation of China under Grants No. 11175095, No. 11205112 and No. 11375094, and by Tsinghua University Initiative Scientific Research Program. The work at Vanderbilt University, Lawrence Berkeley National Laboratory was supported by U. S. Department of Energy under Grant No. DE-FG05-88ER40407 and Contract No. DE-AC03-76SF00098.

[1] L. P. Gaffney et al., Nature 497, 199 (2013), doi:10.1038/nature12073
[2] B. Bucher et al. Phys. Rev. Lett. 116, 112503 (2016).
[3] C. Liu et al., Phys. Rev. Lett. 116, 112501 (2016).
[4] P. A. Butler and W. Nazarewicz, Rev. Mod. Phys. **68**, 349 (1996).
[5] W. Nazarewicz *et al.*, Phys. Rev. Lett. **52**, 1272 (1984).
[6] Z. Sujkowski et al., , Nucl. Phys. A 291, 365 (1977).
[7] D. R. Zolnowski et al., Phys. Lett. B 55, 453 (1975).
[8] D. R. Haenni, and T. T. Sugihara, Phys. Rev. C 16, 120 (1977).
[9] W. R. Phillips *et al.*, Phys. Rev. Lett. **57**, 3257 (1986).
[10] Fernández-Niello et al., Nucl. Phys. A 391, 221 (1982).
[11] D. Ward et al., Nucl. Phys. A 406, 591 (1983).
[12] W. Bonin et al., Z. Phys. 310, 249 (1983).
[13] J. H. Hamilton *et al.*, Prog. Part. Nucl. Phys. **35**, 635 (1995).
[14] S. J. Zhu *et al.*, Phys. Lett. B **357**, 273 (1995).
[15] S. J. Zhu *et al.*, Chin. Phys. Lett. **14**, 569 (1997).
[16] W. Urban *et al.*, Nucl. Phys. A **613**, 107 (1997).
[17] S. J. Zhu *et al.*, Phys. Rev. C **60**, 051304 (1999).
[18] S. J. Zhu *et al.*, Phys. Rev. C **59**, 1316 (1999).
[19] W. R. Phillips *et al.*, Phys. Lett. B **212**, 402 (1988).
[20] L. Y. Zhu *et al.*, High Energy Phys. and Nucl. Phys.-Chinese Edition **22**, 885 (1998).
[21] Y. J. Chen *et al.*, High Energy Phys. and Nucl. Phys.-Chinese Edition **30**, 740 (2006).
[22] Ts. Venkova *et al.*, Eur. Phys. J. A **26**, 315 (2005).
[23] Y. J. Chen *et al.* Phys. Rev. C **73**, 054316 (2006).
[24] S. J. Zhu *et al.*, Phys. Rev. C **85**, 014330 (2012).
[25] H. J. Li *et al.* Phys. Rev. C **90**, 047303 (2014).
[26] H. J. Li *et al.*, Phys. Rev. C **86**, 067302 (2012).
[27] M. Bentaleb *et al.*, Z. Phys. A **345**, 143 (1996).
[28] J. H. Hamilton *et al.*, Prog. Part. Nucl. Phys. **38**, 273 (1997).
[29] W. Urban *et al.*, Eur. Phys. J. A **16**, 303 (2003).
[30] W. Urban *et al.*, Phys. Rev. C **93**, 034326 (2016).
[31] D. C. Radford, Nucl. Instrum. Methods Phys. Res. A **361**, 297 (1995).
[32] S. J. Zhu *et al.*, Int. J. Mod. Phys. E **18** 1717 (2009).
[33] H. B. Ding *et al.*, Phys. Rev. C **77**, 057302 (2008).
[34] S. J. Zhu *et al.*, Phys. Rev. C **65**, 014307 (2001).
[35] I. Deloncle *et al.*, Eur. Phys. J. A **8**, 177 (2000).
[36] A .V. Daniel *et al.*, Nucl. Instrum. Methods B **262**, 399 (2007).
[37] H. W. Taylor, B. Singh, F. S. Prato, and R. McPherson, At. Data Nucl. Data Tables A **9**, 1 (1971).
[38] J. Lange, Krishna Kumar and J. H. Hamilton, Rev. of Mod. Phy. **54**, 119 (1982).
[39] B.B. Fenker, Senior Honor's Thesis, Vanderbilt University, 2010 (to be published).